Institut Riset dan Publikasi Indonesia (IRPI)
IJATIS: Indonesian Journal of Applied Technology and Innovation Science
Journal Homepage: https://journal.irpi.or.id/index.php/ijatis
Vol. 3 Iss. 1 February 2026, pp: 10-18
ISSN(P): 3032-7466 | ISSN(E): 3032-7474

Comparison of Deep Neural Network and Convolutional Neural Network Algorithms for Bone Fracture

Ahmeid Aqeil[1*], Rahmat Afriyanto[2], Arif Haikal Bin Shamsul Kamarul Adzhar[3]

[1,2]Department of Information System, Faculty of Science and Technology,
Universitas Islam Negeri Sultan Syarif Kasim Riau, Indonesia
[3]Department of Computer Science, Faculty of Information and Communication Technology,
International Islamic University Malaysia, Malaysia

E-Mail: [1]12250313332@students.uin-suska.ac.id,
[2]12250314432@students.uin-suska.ac.id, [3]arif.h@live.iium.edu.my

Received Aug 20th 2025; Revised Mar 05th 2026; Accepted Mar 15th 2026; Available Online Mar 16th 2025
Corresponding Author: Ahmeid Aqeil
Copyright © 2026 by Authors, Published by Institut Riset dan Publikasi Indonesia (IRPI)

Abstract

Bone fracture is a common medical condition that often affects elderly populations or individuals with degenerative diseases such as osteoporosis. Manual classification of fractures from X-ray images presents diagnostic challenges due to visual complexity and interobserver variability. In this study, we implemented and compared Deep Neural Network (DNN) and Convolutional Neural Network (CNN) architectures to classify bone fractures from radiographic images. The dataset consisted of 4099 X-ray images divided into fractured and non-fractured categories. Each model was trained using preprocessed and augmented data and evaluated using accuracy, precision, recall, and F1-score metrics. The evaluation results showed that the CNN model achieved better classification performance, with an accuracy of 80% and balanced class scores. In contrast, the DNN model showed poor generalization and strong bias toward the fractured class, yielding only 51% accuracy. This study concludes that CNN are more suitable for bone fracture classification tasks due to their superior ability to extract spatial features and generalize across categories.

Keywords: Bone Fracture, Deep Neural Network, Convolutional Neural Network, Medical Image Classification

1. INTRODUCTION

Bone fractures are one of the most common medical conditions, especially in the elderly population and patients with degenerative diseases such as osteoporosis [1]. Proper identification and classification of fractures is essential to determine optimal treatment [2],[3],[4]. However, conventional approaches through interpretation of medical images (e.g., radiographs or CT scans) often rely on radiologic expertise that is not always equally available, and may introduce inter-examiner variability [5].

In clinical practice, the classification of bone fractures based on medical images such as X-rays or CT scans still relies heavily on manual interpretation by radiologists or orthopedists [3], [4]. The main problems that arise are the limited number of experts in first-level health facilities, as well as the potential for interobserver variability in diagnosis, which can affect the accuracy of determining the type and location of the fracture [5], [6], [7]. In addition, fracture images are often complex, visually overlapping with soft tissue, or of low quality, compounding the identification challenge [8], [9]. This makes fracture classification a real challenge that requires technology-based automated solutions to ensure accuracy and speed in clinical decision-making [9], [10].

In recent years, advances in artificial intelligence (AI) technology, particularly Deep Learning (DL), have brought about a transformation in medical image analysis [11], [12]. Two main approaches in DL, namely Deep Neural Network (DNN) and Convolutional Neural Network (CNN), have shown high performance in detecting and classifying abnormalities in medical images with accuracy approaching, even exceeding, the performance level of human clinicians [13], [14]. CNN is particularly effective in image data processing due to its ability to extract spatial features, while DNN excels in complex classification processes based on processed feature vectors [8], [15], [16].

Several previous studies have applied deep learning models, especially CNNs, to classify bone fractures, such as those of the vertebrae, extremities, or pelvis, and have shown promising results in image-based

automatic detection [9], [17], [18]. In addition, one study developed an Artificial Neural Network (ANN) model using 20 input features to predict hospitalization duration, intensive care unit stay, survival rate, and mortality in patients with rib fractures [19]. In a recent study, an approach combining DenseNet201 and VGG16, achieving 97% accuracy during the validation phase, accurately identified and classified different types of fractures [8], [20].

Another study proposed a TandemNet approach that integrates natural language understanding with musculoskeletal image analysis, to improve the accuracy and interpretability of deep learning models through the incorporation of visual and textual information from medical reports [21], [22]. Meanwhile, in a study that designed a Recurrent Neural Network (RNN) model with a visual attention mechanism, which is able to focus on critical areas in medical images to detect bone fractures more efficiently and precisely [23], [24].

This study aims to build and compare DNN- and CNN-based bone fracture prediction models using split classification. The main contribution of this study is the exploration of a model architecture that can handle the complexity of medical image features while providing specific classification outputs for fracture categories. This study also proposes an integrative approach combining DNN and CNN to improve the model's accuracy and interpretability, aiming to address a gap in the literature on the application of DL for precise fracture prediction.

2. MATERIAL AND METHOD

The process begins with the collection of X-ray image data, which is the main material for model training. Next, a preprocessing stage is performed to improve image quality and prepare the images in a format suitable for the model. After that, the processed images undergo an augmentation stage to increase data diversity and reduce the risk of overfitting during training. The augmented data is then used to train two types of models, namely DNN and CNN, each with a different approach to identifying characteristics in images. The next stage is model evaluation using performance metrics. The process ends once the evaluation demonstrates that the model has attained the desired performance.

The research methodology diagram is observable in Figure 1.

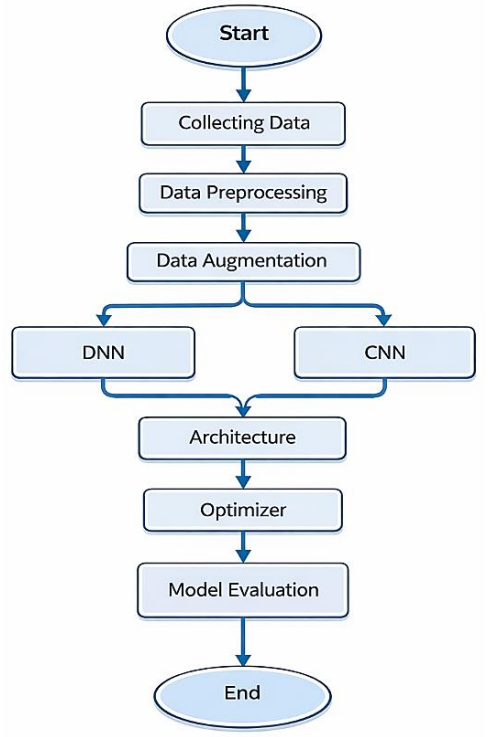

Figure 1. Research Methodology

2.1. Deep Learning

Deep learning is an advanced development of machine learning that uses layered artificial neural networks to learn hierarchical representations of data, ranging from simple perceptron models to complex architectures such as CNN, SAE, DBN, and DBM, as well as generative innovations such as GAN [25], [26]. These methods show significant advantages in speech and image recognition that require large data and intensive computation, with wide applications in computer vision, natural language processing, and medical analysis [27]. Therefore, future research is directed towards developing more efficient architectures,

interpretability techniques, and training methods that address complexity and maintain security and fairness in the use of deep learning [28].

2.2. Deep Neural Network (DNN)

DNN is an architecture that consists of multiple hidden layers and is able to learn non-linear patterns from input data through a structured training process [29]. The network works by gradually transforming the data in each layer to produce an optimal feature representation to support the final classification [30], [31]. In this study, DNN is trained using a dataset that has been processed through the stages of image augmentation and normalization, then optimized using the backpropagation algorithm and ReLU activation function for each hidden layer [32].

2.3. Convolutional Neural Network (CNN)

CNNs are purpose-built to process grid-shaped data like images, by utilizing convolution layers followed by pooling operations, as well as non-linear activation functions for the purpose of producing deeper and more meaningful feature representations [33], [34], [35]. The CNN model is made up of several convolution blocks, each followed by batch normalization and max pooling, and ends with two classes classified using a fully connected layer: broken and unbroken [36]. The CNN is trained using X-ray image data that has been quality-enhanced through histogram equalization and augmentation to prevent overfitting [37].

2.4. MobileNetV2

MobileNetV2 is a CNN architecture from Google, designed for mobile devices and embedded systems with limited computation [38]. It balances accuracy and model size through optimizations such as depthwise separable convolution, which splits the convolution into depthwise and pointwise stages for efficiency, and linear bottleneck, which reduces feature dimensions and computation using fewer filters [39]. The basic unit is the inverted residual block, which combines convolution, batch normalization, and shortcut connections [40]. As a result, MobileNetV2 performs well for identifying objects and categorizing images with a smaller model and lower computation than conventional CNNs, making it ideal for limited power devices [38].

2.5. Adam

Adam optimizer is an optimization algorithm developed from stochastic gradient descent by combining the benefits of AdaGrad and RMSProp, so that it is able to adaptively adjust the per-parameter learning level based on the mean of previous gradients and gradient moments [41]. Adam is computationally efficient and requires relatively small memory, making it suitable for deep learning models with large datasets and sparse gradient and noisy problems [42]. Adam's advantages include fast convergence, automatic learning rate adaptability, and generally better performance than other optimizers such as SGD and RMSProp [43]. However, the drawbacks are that sometimes Adam can produce poor generalization in some cases and sensitivity to hyperparameter settings such as learning level and beta decay value that require further tuning to be optimal [44].

3. RESULTS AND DISCUSSION

At this phase, the outcome of the bone fracture image classification process using CNN are analyzed. The previous process began with data collection, preprocessing, and the use of the hold-out method to split the data. Next, the DNN model is optimized with the ADAM optimizer, while the CNN model is built using the MobileNetV2 architecture and optimized with the ADAM optimizer. An evaluation is conducted To assess the performance of the combination of architecture and optimizer in categorizing bone fracture condition images.

3.1. Collecting Data

The data taken showing the x-ray condition of the bone that is broken or not in this study is obtained from the Kaggle platform and is owned by [45]. The dataset used has 2 classes, namely fractured or not fractured, with each class consisting of 2020 images and 2079 images, totaling 4099 images. Details can be seen in Table 1.

Table 1. Details of x-ray dataset count

Class	Number of Datasets
Fracture	2020
Not Fracture	2079

3.2. Preprocessing

In the preprocessing step, all pictures were resized to a uniform 150x150 pixels and scaled to the range 0-1. To increase the diversity of the training data and prevent overfitting, data augmentation techniques like random rotation of up to 30 degrees, horizontal and vertical position shifts of 10% of the image dimensions

each, shear transformation, zoom of up to 20%, and horizontal inversion were applied. In addition, a hold-out validation method was used, with 20% of the data set aside for validation. The augmented image is shown in Figure 2.

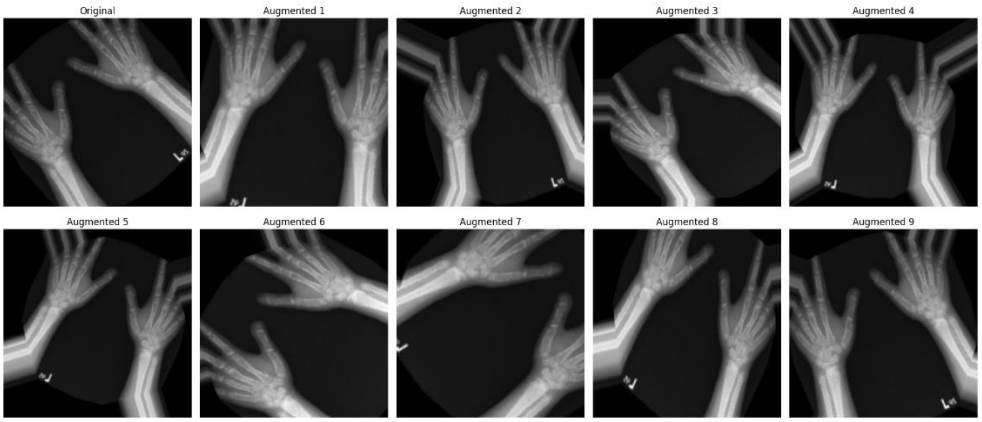

Figure 2. Result Augmentation

3.3. Training Process

This research implements two deep learning architectures, namely DNN and CNN, to classify fractures. Data sharing occurs at the beginning, followed by the augmentation of the dataset images for later use. A DNN with a simple non-convolutional design is used. The input image was first flattened, then passed to two dense layers (256 and 128 units) with ReLU activation. Dropout regularization (0.3) is applied after each dense layer to mitigate overfitting. The final output layer uses softmax activation with the same number of neurons as the number of target classes for probability prediction. The model training configuration involves the Adam optimizer, categorical cross-entropy loss function, and accuracy metric.

Table 2 shows the results of the DNN Model Evaluation.

Table 2. DNN Model Evaluation Results

Class	Precision	Recall	F1-Score	Support
Fractured	0.51	1.00	0.67	41
Not Fractured	0.00	0.00	0.00	40
Accuracy			0.51	81
Macro Avg	0.25	0.50	0.34	81
Weighted Avg	0.26	0.51	0.34	81

The evaluation of the DNN model revealed a modest accuracy of 51% on the validation dataset. While the model demonstrated a commendable ability to identify all instances of fractured images, achieving perfect recall (1.00) for this class, its precision was limited to 0.51. This suggests that a significant proportion, indeed over half, of the predictions categorized as "broken" were, in fact, misclassified. Conversely, the model performance on the "not fractured" class was notably deficient, as indicated by precision, recall, and F1-score values of 0.00. This effectively indicates the model's inability to recognize this particular class. The overall challenge the DNN model faced in distinguishing equitably between the two classes within the validation data is further underscored by the weighted average and macro average F1-scores, both of which settled at a relatively low 0.34.

Concurrently, a CNN architecture was designed, incorporating a series of convolutional layers specifically to discern and extract salient spatial features from the input images. This model architecture strategically employs the Rectified Linear Unit (ReLU) as its activation function. It is structured with three sequential convolutional blocks, featuring 32, 64, and 128 filters of a 3x3 kernel size, respectively. Following each of these convolutional blocks, a 2x2 max pooling layer is implemented to systematically reduce the spatial dimensionality of the feature maps. Upon the successful extraction of these features, the resultant output is transformed into a one-dimensional vector via a Flatten layer. This flattened representation is then processed by a densely connected layer comprising 128 neurons, with a dropout rate of 0.3 to mitigate overfitting. The architecture culminates in an output layer that utilizes a softmax activation function, enabling it to generate predictions suitable for a multiclass classification task. For the training process, the Adam optimization algorithm was selected, and this model was developed using categorical cross-entropy as the loss function, with accuracy as the main metric for performance evaluation.

Table 3. CNN Model Evaluation Results

Class	Precision	Recall	F1-Score	Support
Fractured	0.84	0.76	0.79	41
Not Fractured	0.77	0.85	0.81	40
Accuracy			0.80	81
Macro Avg	0.81	0.80	0.80	81
Weighted Avg	0.81	0.80	0.80	81

Analysis of the validation dataset reveals that the CNN architecture outperforms the preceding DNN model, particularly in achieving a more balanced and accurate classification. For the 'fractured' class, the CNN model attained a precision of 0.84, a recall of 0.76, and an F1-score of 0.79. These metrics indicate that, although some misclassifications persisted, the model was largely successful at correctly identifying images of fractures.

Meanwhile, for the 'not fractured' class, the model demonstrated a distinct performance profile, achieving a precision of 0.77 and a recall of 0.85. These figures illustrate that most images without fractures were accurately identified, even though some instances within this class were not perfectly captured. The overall robustness of the model is further substantiated by achieving identical macro and weighted average F1-scores of 0.80, and an overall system accuracy of 80%. Collectively, these results indicate the model's excellent, reliable ability to differentiate between the two image categories.

To analyze the training performance more thoroughly, see Figures 3 and 4.

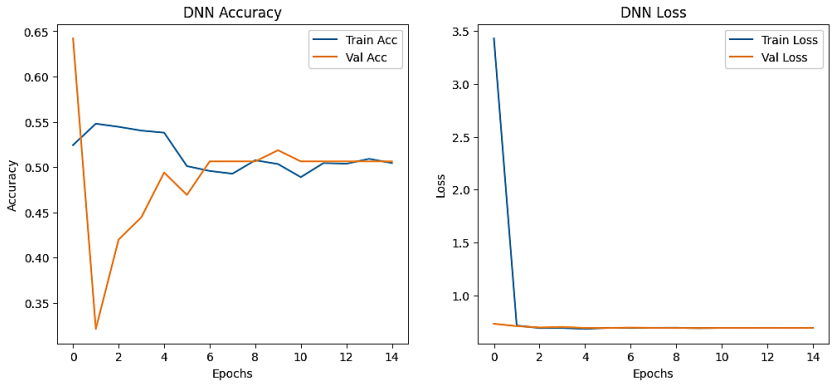

Figure 3. Training and Validation Accuracy DNN

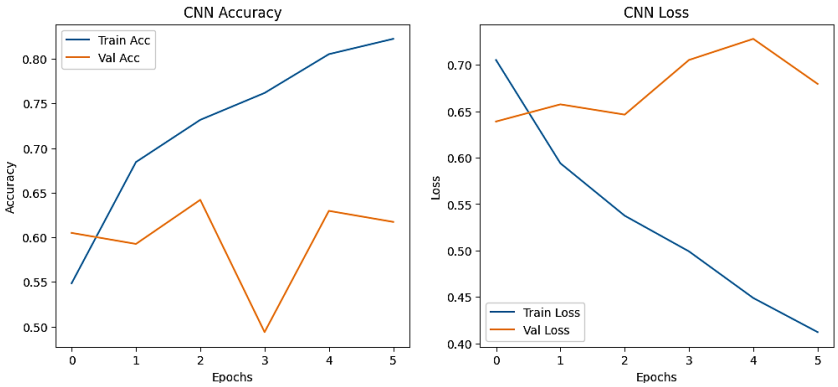

Figure 4. Training and Validation Accuracy CNN

Based on the accuracy and loss graphs in Figure 4, the CNN model shows better performance than the DNN model in Figure 3. CNN shows a consistent increase in accuracy, with a small difference between training and validation accuracy, and a steady decrease in loss, indicating good generalization. In contrast, DNN shows fluctuations in validation accuracy and a large initial loss difference, indicating low learning efficiency and potential underfitting. To provide a clearer picture of the classification performance of the two algorithms, Figures 5 and 6 show the confusion matrix of the DNN and CNN algorithms, respectively.

The confusion matrix of the CNN algorithm shows good classification performance, with most of the data being classified correctly. This can be seen from the high main diagonal values, where 31 fractured samples and 34 not fractured samples were correctly predicted. However, there are still misclassifications, such as 10 fractured samples predicted as not fractured, and 6 not fractured samples predicted as fractured. Overall,

the CNN model showed a balanced performance with an accuracy of 80%, as reflected in the near-ideal prediction distribution.

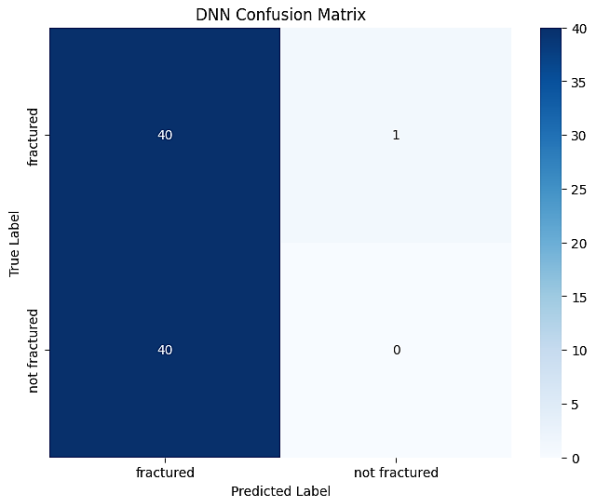

Figure 5. Confusion Matrix DNN

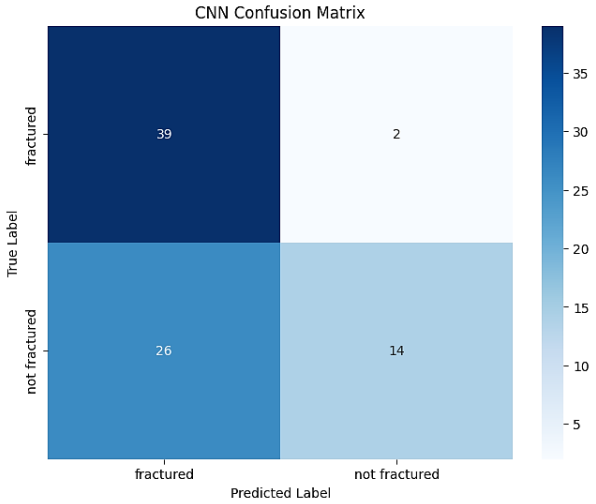

Figure 6. Confusion Matrix CNN

In contrast, the DNN algorithm consistently predicted all images as “fractured,” with no predictions for the “not fractured” class. This is demonstrated by 41 “fractured” samples being correctly classified, but all 40 “not fractured” samples being misclassified as “fractured”, resulting in a very high false positive rate. This imbalance indicates that the model suffers from extreme bias towards one class, which could be caused by issues in the training data distribution, a suboptimal training process, or an inappropriate model architecture. As a result, the model's accuracy reached only 51%, and although it appeared high for one class, its overall performance in distinguishing between the two was very low.

Overall, CNN performed better than DNN in terms of fracture image classification, with more balanced and accurate precision, recall, and f1-score values. This shows that CNN is better at distinguishing visual features in the image than DNN, as illustrated in the confusion matrices for each model.

4. CONCLUSION

After comparing the performance of DNN and CNN at classifying bone fracture conditions based on X-ray images. The DNN model, despite its simple architecture, failed to generalize well and showed extreme bias toward the fractured class, misclassifying all non-fractured images. The accuracy of this model only reached 51%. In contrast, the CNN model performed much better, achieving 80% accuracy, balanced recall and precision across both classes, and a more representative confusion matrix. These findings suggest that CNNs are more appropriate for medical image classification tasks, particularly for bone fracture identification. Future research could explore the adoption of architecture optimization techniques to improve accuracy and reduce error rates in a broader clinical context.

REFERENCES

[1] A. I. Hormigo-Sánchez, M. Neira-Álvarez, and T. Pareja-Sierra, "Approach to the elderly patient with vertebral fracture due to bone fragility," Rev. Esp. Cir. Ortop. Traumatol., Nov. 2024, doi: 10.1016/j.recot.2024.03.011.

[2] E. Şahin, "A new radiographic classification of fifth distal metacarpal fractures," Irish J. Med. Sci. (1971 -), vol. 191, no. 3, pp. 1355–1360, 2022, doi: 10.1007/s11845-021-02684-2.

[3] W. Hintringer et al., "Biomechanical considerations on a CT-based treatment-oriented classification in radius fractures," Arch. Orthop. Trauma Surg., vol. 140, no. 5, pp. 595–609, May 2020, doi: 10.1007/s00402-020-03405-7.

[4] H. Sri and S. Rethinavalli, "Deep Learning For Bone Fracture Detection: A Survey And Comparative Study," Int. J. Creat. Res. THOUGHTS, vol. 12, p. a898, Oct. 2024.

[5] A. Alam et al., "Novel transfer learning based bone fracture detection using radiographic images," BMC Med. Imaging, vol. 25, no. 1, Jan. 2025, doi: 10.1186/s12880-024-01546-4.

[6] G. González et al., "Classification and segmentation of hip fractures in x-rays: highlighting fracture regions for interpretable diagnosis," Insights Imaging, vol. 16, no. 1, Apr. 2025, doi: 10.1186/s13244-025-01958-y.

[7] L. Mattijssen-Horstink, J. J. Langeraar, G. J. Mauritz, W. Van Der Stappen, M. Baggelaar, and E. C. T. H. Tan, "Radiologic discrepancies in diagnosis of fractures in a Dutch teaching emergency department: A retrospective analysis," Scand. J. Trauma. Resusc. Emerg. Med., vol. 28, no. 1, May 2020, doi: 10.1186/s13049-020-00727-8.

[8] T. Aldhyani et al., "Diagnosis and detection of bone fracture in radiographic images using deep learning approaches," Front. Med., vol. 11, 2024, doi: 10.3389/fmed.2024.1506686.

[9] J. D. Krogue et al., "Automatic hip fracture identification and functional subclassification with deep learning," Radiol. Artif. Intell., vol. 2, no. 2, 2020, doi: 10.1148/RYAI.2020190023.

[10] Y. L. Thian, Y. Li, P. Jagmohan, D. Sia, V. E. Yao Chan, and R. T. Tan, "Convolutional neural networks for automated fracture detection and localization on wrist radiographs," Radiol. Artif. Intell., vol. 1, no. 1, Jan. 2019, doi: 10.1148/ryai.2019180001.

[11] M. Xu and C. Jia, "Application of artificial intelligence technology in medical imaging," in Journal of Physics: Conference Series, IOP Publishing Ltd, Oct. 2021. doi: 10.1088/1742-6596/2037/1/012090.

[12] E. Sudheer Kumar and C. Shoba Bindu, "Medical Image Analysis Using Deep Learning: A Systematic Literature Review," in Emerging Technologies in Computer Engineering: Microservices in Big Data Analytics, A. K. Somani, S. Ramakrishna, A. Chaudhary, C. Choudhary, and B. Agarwal, Eds., Singapore: Springer Singapore, 2019, pp. 81–97.

[13] S. Serte, A. Serener, and F. Al-Turjman, "Deep learning in medical imaging: A brief review," Trans. Emerg. Telecommun. Technol., vol. 33, no. 10, p. e4080, Oct. 2022, doi: https://doi.org/10.1002/ett.4080.

[14] M. A. Mazurowski, M. Buda, A. Saha, and M. R. Bashir, "Deep learning in radiology: An overview of the concepts and a survey of the state of the art with focus on MRI," Apr. 01, 2019, John Wiley and Sons Inc. doi: 10.1002/jmri.26534.

[15] D. Hemanand, B. N. P. G., A. Shahanaz, A. Mohd Wazih, N. S., and A. and Haldorai, "Multilayer vectorization to develop a deeper image feature learning model," Automatika, vol. 64, no. 2, pp. 355–364, Apr. 2023, doi: 10.1080/00051144.2022.2157946.

[16] S. Ramasamy and M. Perumal, "CNN-based deep learning technique for improved H7 TLI with grid-connected photovoltaic systems," Int. J. Energy Res., vol. 45, no. 14, pp. 19851–19868, Nov. 2021, doi: https://doi.org/10.1002/er.7030.

[17] M. Kutbi, "Artificial Intelligence-Based Applications for Bone Fracture Detection Using Medical Images: A Systematic Review," Diagnostics, vol. 14, no. 17, p. 1879, Aug. 2024, doi: 10.3390/diagnostics14171879.

[18] Y. Li et al., "Differential diagnosis of benign and malignant vertebral fracture on CT using deep learning," Eur. Radiol., vol. 31, no. 12, pp. 9612–9619, 2021, doi: 10.1007/s00330-021-08014-5.

[19] R. Ippoliti, G. Falavigna, C. Zanelli, R. Bellini, and G. Numico, "Neural networks and hospital length of stay: an application to support healthcare management with national benchmarks and thresholds," Cost Eff. Resour. Alloc., vol. 19, no. 1, Dec. 2021, doi: 10.1186/s12962-021-00322-3.

[20] F. Yang, R. Cong, M. Xing, and B. Ding, "Study on AO classification of distal radius fractures based on multi-feature fusion," in Journal of Physics: Conference Series, IOP Publishing Ltd, Feb. 2021. doi: 10.1088/1742-6596/1800/1/012006.

[21] G. Chauhan et al., "Joint Modeling of Chest Radiographs and Radiology Reports for Pulmonary Edema Assessment," in Lecture Notes in Computer Science (including subseries Lecture Notes in Artificial Intelligence and Lecture Notes in Bioinformatics), Springer Science and Business Media Deutschland GmbH, 2020, pp. 529–539. doi: 10.1007/978-3-030-59713-9_51.

[22] Fabio Galbusera, Andrea Cina, Tito Bassani, Matteo Panico, and Luca Maria Sconfienza,

"Automatic Diagnosis of Spinal Disorders on Radiographic Images: Leveraging Existing Unstructured Datasets With Natural Language Processing," Glob. Spine J., vol. 13, no. 5, pp. 1257–1266, Jul. 2021, doi: 10.1177/21925682211026910.

[23] C.-T. Chien, R.-Y. Ju, K.-Y. Chou, E. Xieerke, and J.-S. Chiang, "YOLOv8-AM: YOLOv8 Based on Effective Attention Mechanisms for Pediatric Wrist Fracture Detection," Feb. 2024, [Online]. Available: http://arxiv.org/abs/2402.09329

[24] Xiaoning Cui, Qicai Wang, Jinpeng Dai, Yanjin Xue, and Yun Duan, "Intelligent crack detection based on attention mechanism in convolution neural network," Adv. Struct. Eng., vol. 24, no. 9, pp. 1859–1868, Jan. 2021, doi: 10.1177/1369433220986638.

[25] M. Vogt, "An Overview of Deep Learning and Its Applications BT - Fahrerassistenzsysteme 2018," T. Bertram, Ed., Wiesbaden: Springer Fachmedien Wiesbaden, 2019, pp. 178–202.

[26] L. Alzubaidi et al., Review of deep learning: concepts, CNN architectures, challenges, applications, future directions, vol. 8, no. 1. Springer International Publishing, 2021. doi: 10.1186/s40537-021-00444-8.

[27] Q. Kong, Y. Cao, T. Iqbal, Y. Wang, W. Wang, and M. D. Plumbley, "PANNs: Large-Scale Pretrained Audio Neural Networks for Audio Pattern Recognition," IEEE/ACM Trans. Audio, Speech and Lang. Proc., vol. 28, pp. 2880–2894, Nov. 2020, doi: 10.1109/TASLP.2020.3030497.

[28] A. Pramod, H. S. Naicker, and A. K. Tyagi, "Machine Learning and Deep Learning: Open Issues and Future Research Directions for the Next 10 Years," in Computational Analysis and Deep Learning for Medical Care, 2021, pp. 463–490. doi: https://doi.org/10.1002/9781119785750.ch18.

[29] M. Madhiarasan and M. Louzazni, "Analysis of Artificial Neural Network: Architecture, Types, and Forecasting Applications," J. Electr. Comput. Eng., vol. 2022, no. 1, p. 5416722, Jan. 2022, doi: https://doi.org/10.1155/2022/5416722.

[30] S. H. Kong et al., "A Computed Tomography–Based Fracture Prediction Model With Images of Vertebral Bones and Muscles by Employing Deep Learning: Development and Validation Study," J. Med. Internet Res., vol. 26, no. 1, 2024, doi: 10.2196/48535.

[31] A. Alshahrani and A. Alsairafi, "Bone Fracture Classification using Convolutional Neural Networks from X-ray Images," Eng. Technol. Appl. Sci. Res., vol. 14, no. 5, pp. 16640–16645, Oct. 2024, doi: 10.48084/etasr.8050.

[32] N. V. Sridharan and V. and Sugumaran, "Convolutional Neural Network based Automatic Detection of Visible Faults in a Photovoltaic Module," Energy Sources, Part A Recover. Util. Environ. Eff., vol. 47, no. 1, pp. 6270–6284, Dec. 2025, doi: 10.1080/15567036.2021.1905753.

[33] T. H. Yang, M. H. Horng, R. S. Li, and Y. N. Sun, "Scaphoid Fracture Detection by Using Convolutional Neural Network," Diagnostics, vol. 12, no. 4, Apr. 2022, doi: 10.3390/diagnostics12040895.

[34] Z. Liao et al., "CNN Attention Guidance for Improved Orthopedics Radiographic Fracture Classification," Mar. 2022, doi: 10.1109/JBHI.2022.3152267.

[35] D. Chettrit et al., "3D Convolutional Sequence to Sequence Model for Vertebral Compression Fractures Identification in CT," Oct. 2020, [Online]. Available: http://arxiv.org/abs/2010.03739

[36] W. Huang, Q. Wenli, and P. and Ge, "Orthogonal tests investigation into hybrid fiber-reinforce recycled aggregate concrete and convolutional neural network prediction," J. Asian Archit. Build. Eng., vol. 21, no. 3, pp. 986–1001, May 2022, doi: 10.1080/13467581.2021.1918553.

[37] T. Dorosti et al., "Optimizing convolutional neural networks for Chronic Obstructive Pulmonary Disease detection in clinical computed tomography imaging," Comput. Biol. Med., vol. 185, p. 109533, 2025, doi: https://doi.org/10.1016/j.compbiomed.2024.109533.

[38] D. Qin et al., "MobileNetV4: Universal Models for the Mobile Ecosystem BT - Computer Vision – ECCV 2024," A. Leonardis, E. Ricci, S. Roth, O. Russakovsky, T. Sattler, and G. Varol, Eds., Cham: Springer Nature Switzerland, 2025, pp. 78–96.

[39] Y. Xiong et al., "MobileDets: Searching for Object Detection Architectures for Mobile Accelerators," Proc. IEEE Comput. Soc. Conf. Comput. Vis. Pattern Recognit., pp. 3824–3833, 2021, doi: 10.1109/CVPR46437.2021.00382.

[40] D. Li et al., "Involution: Inverting the inherence of convolution for visual recognition," Proc. IEEE Comput. Soc. Conf. Comput. Vis. Pattern Recognit., pp. 12316–12325, 2021, doi: 10.1109/CVPR46437.2021.01214.

[41] J. Yun, "Stochastic gradient sampling for enhancing neural networks training," Neural Comput. Appl., May 2025, doi: 10.1007/s00521-025-11242-1.

[42] N. Xiao, X. Liu, X. Hu, and K.-C. Toh, "Adam-family Methods for Nonsmooth Optimization with Convergence Guarantees Xiaoyin Hu * Kim-Chuan Toh," 2024. [Online]. Available: http://jmlr.org/papers/v25/23-0576.html.

[43] R. M. Schmidt, F. Schneider, and P. Hennig, "Descending through a Crowded Valley -- Benchmarking Deep Learning Optimizers," 2021.

[44] Q. Tong, G. Liang, and J. Bi, "Calibrating the adaptive learning rate to improve convergence of

ADAM," Neurocomputing, vol. 481, pp. 333–356, 2022, doi: https://doi.org/10.1016/j.neucom.2022.01.014.
[45] Ahmed Ashraf, "Bone Fracture," Kaggle. Accessed: May 14, 2025. [Online]. Available: https://www.kaggle.com/datasets/ahmedashrafahmed/bone-fracture